Systematic behaviour in trivalent lanthanide charge transfer energies

2003 J. Phys.: Condens. Matter 15 8417

(http://iopscience.iop.org/0953-8984/15/49/018)

INSTITUTE OF PHYSICS PUBLISHING JOURNAL OF PHYSICS: CONDENSED MATTER

J. Phys.: Condens. Matter **15** (2003) 8417–8434 PII: S0953-8984(03)68510-3

Systematic behaviour in trivalent lanthanide charge transfer energies

P Dorenbos

Interfaculty Reactor Institute, Delft University of Technology, Mekelweg 15, 2629 JB Delft, The Netherlands

E-mail: dorenbos@iri.tudelft.nl

Received 1 September 2003
Published 25 November 2003
Online at stacks.iop.org/JPhysCM/15/8417

Abstract

Information on the energy that is needed to transfer an electron from the valence band of an inorganic compound to a trivalent lanthanide impurity is presented. The energy is a measure of the location of the ground state of the divalent lanthanide relative to the top of the valence band. A variation with type of lanthanide is found that is the same irrespective of the type of compound (fluorides, chlorides, bromides, iodides, oxides, sulfides). The variation is anti-correlated with the known variation in fd transition energies in divalent lanthanides. Because of the anti-correlation, the energy difference between the first $4f^{n-1}5d$ state and the bottom of the conduction band is relatively invariant with type of lanthanide ion. The difference is largest for Eu^{2+}, and decreases gradually towards the end of the lanthanide series by 0.5 eV for Yb^{2+}. Based on the systematic variation in charge transfer energy and fd energy, a three-parameter model is presented to position the energy levels for each divalent lanthanide relative to valence and conduction band states. Using a similar model the levels of trivalent lanthanides are positioned.

(Some figures in this article are in colour only in the electronic version)

1. Introduction

The location of lanthanide impurity levels relative to the valence band and conduction band in inorganic compounds is important for the performance of materials in applications. A few tenths of electronvolts shift may turn it from bad to good. For example, the dipole allowed df luminescence of Ce^{3+} utilized in scintillator applications but also that of Eu^{2+} in luminescent phosphors can only be efficient when autoionization of the excited 5d electron to conduction band levels is improbable [1, 2]. The minimal energy E_{dC} needed to ionize the 5d electron (d) to the conduction band (C) is then an important parameter. Excited state absorption (ESA) to conduction band states is an energy loss mechanism in high power laser applications [3, 4]. The

0953-8984/03/498417+18$30.00

chemical stability of lanthanides against reduction or oxidation and the ability of lanthanide ions to trap an electron from the conduction band or a hole from the valence band are both determined by impurity level positions. Knowledge of these positions is a first requirement to understand the mechanisms of charge trapping and transport phenomena in scintillators [5], persistent afterglow materials [6, 7], storage phosphors [8], and optical memories [9, 10].

There are several approaches to determine impurity level positions. With ultraviolet photoelectron spectroscopy (UPS) and x-ray photoelectron spectroscopy (XPS), the energy difference between the localised $4f^n$ ground state level and the delocalized valence band levels can be determined [5, 11–14]. With photoconductivity measurements the energy difference with the bottom of the conduction band can be determined [15, 16], and with excited state absorption (ESA) or luminescence quenching studies information on the transitions from the excited 5d level to conduction band levels can be obtained [2, 17].

There are other indirect means. For divalent lanthanides with lowest 5d level close to the bottom of the conduction band, the 5d electron may autoionize to conduction band states. The Coulomb attraction with the hole left behind leads to a bound electron Ln^{3+} state, also known as an impurity trapped exciton [18]. The radiative return to the $4f^n$ ground state of Ln^{2+} is known as anomalous emission. The probability for this to occur as a function of type of divalent lanthanide and type of host crystal has provided qualitative information on the change in the 5d ionization energy E_{dC} with type of lanthanide and with type of host crystal [19]. It was concluded that E_{dC} for Yb^{2+} is always smaller than for Eu^{2+}. Also clear trends with the type of compound, i.e., the site occupied, the type of anions, and the binding of the upper valence band electrons, were found.

To understand these trends three interactions were considered.

(1) The changing Madelung potential and electron–electron repulsion at the lanthanide site due to lattice relaxation,
(2) the isotropic exchange interaction between 5d electron spin and total $4f^{n-1}$ electron spin, and
(3) the Coulomb interaction between the 5d electron and the $Ln^{3+}[Xe]4f^{n-1}$ core.

These three interactions create a variation of E_{dC} with type of lanthanide ion, such as is shown in figure 1. Arrow 1 indicates the ionization of the 5d electron in Dy^{2+}. From La^{2+} to Gd^{2+}, the ionization energy E_{dC} is relatively constant, and from Gd^{2+} to Yb^{2+} E_{dC} it decreases by $\approx$0.5 eV. If we add information on the systematic variation in the fd transition energies of divalent lanthanides from [20] one may position the lowest $4f^n$ state for each lanthanide as illustrated by the curve labelled $4f^n$ in figure 1.

The three interactions qualitatively explain the trends found but they do not allow for an absolute determination of the magnitude of E_{dC}. The aim of this paper is to provide experimental data for this absolute location. This is done by studying the energy of the charge transfer bands of trivalent lanthanides. An electron from the valence band is transferred to the trivalent lanthanide ion and Ln^{2+} is created. Somehow, the CT energy is related to the energy difference between the valence band and the ground state of the divalent lanthanide [21–23].

This paper is organized as follows. First a general treatment of the charge transfer and possible pitfalls in its interpretation is presented. Information on charge transfer energies for the trivalent lanthanides in compounds obtained from literature is presented next. It is concluded that, despite the complex nature of the CT transition, the CT energy provides a fair measure of the location of the Ln^{2+} ground state above the top of the valence band. Since the interest is in how it changes with type of lanthanide, analysis is limited to compounds with CT information on at least two different lanthanides. A systematic change in CT energy with type of lanthanide was revealed a long time ago for bromide complexes of trivalent Sm, Eu, Tm, and

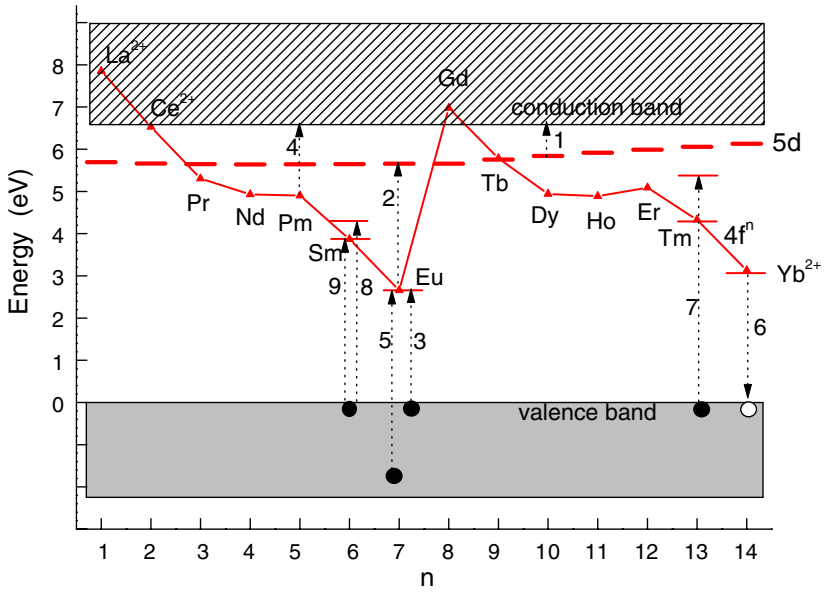

Figure 1. The systematic variation in the energy level positions of divalent lanthanides in wide band gap ionic crystals. n represents the number of electrons in the $4f^n5d^0$ configuration of the divalent lanthanide. Arrows indicate possible electron transitions discussed in the text.

Yb in ethanol by Jörgensen [24]. Barnes and Pincott [25] and also Blasse and Bril [26] found that the CT band of Sm^{3+} in solids appears always 1.1 ± 0.1 eV higher in energy than that of Eu^{3+}. More recent studies were done by Krupa and co-workers [27, 28], and van Pieterson and co-workers [29, 30] compared the CT band energies of Yb^{3+} with that of Eu^{3+}.

In the present work the study covers a much wider collection of compounds and to all lanthanides for which information is available. The systematic variation with type of lanthanide appears not to depend on type of compound. Furthermore, the trends and conclusions from the study of anomalous emission is confirmed by the study on CT energies [19]. Finally, a model is presented to draw the energy level positions for each divalent lanthanide. The model contains three host dependent parameters: (1) the band gap of the host compound, (2) the CT energy for Eu^{3+}, and (3) the redshift of the fd transition in that compound.

2. The nature of the CT band

A generalized notation is used where level energies are expressed as a function of the ionic charge Q of the lanthanide ion, the number of electrons n in the $4f^n5d^0$ configuration, and the type of compound designated by the parameter A. In this notation $E^{CT}(6, 3+, A)$ means the energy of the charge transfer band of Eu^{3+} ($n = 6$) in compound A. Arrow 3 in figure 1 illustrates this transition, which starts from the top of the valence band and ends in the ground state of Eu^{2+}. The superscript CT indicates the type of transition. pc is, for example, used for the photoconductivity threshold and fa for the energy of the fundamental absorption threshold. $E_{fd}(7, 2+, A)$ is the energy for the transition from the first $4f^n$ level to the first $4f^{n-1}5d$ level in Eu^{2+} which is illustrated by arrow 2. The subscript fd indicates the transition from f to d. $E_{fC}(5, 2+, A)$ is the energy difference between the $4f^5$ ground state of Pm^{2+} and the bottom of the conduction band (C); see arrow 4. $E_{Vf}(7, 2+, A)$ is the energy difference between the top of the valence band (V) and the $4f^7$ ground state of Eu^{2+}.

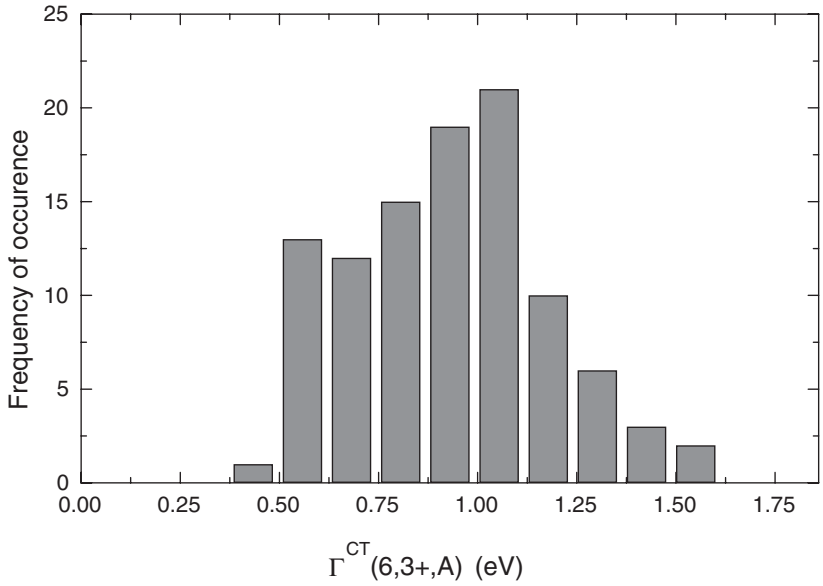

Figure 2. A histogram of the distribution of the width (FWHM) $\Gamma^{CT}(6, 3+, A)$ of the charge transfer band of Eu^{3+} in compounds. The data are from [37].

The energy for the first fd transition of lanthanides in compounds is related as [20, 31]

$$E_{fd}(n, Q, A) = E_{Afree}(n, Q) - D(Q, A) \tag{1}$$

where $E_{Afree}(n, Q)$ are constants with values close to the first fd transition energy in the free lanthanide ions. The redshift $D(Q, A)$ is the amount by which the 5d level shifts towards lower energy when the lanthanide is incorporated in a compound. This shift is within 0.1 eV the same for each lanthanide when in the same site in the same compound [31, 20]. Knowledge of either $E_{dC}(n, 2+, A)$ or $E_{fC}(n, 2+, A)$ for each n together with $D(2+, A)$ is needed to draw the energy levels for each lanthanide in schemes like figure 1.

The charge transfer from the valence band to a trivalent lanthanide appearing as an intense band in absorption, excitation, and reflection spectra is due to a spin and dipole allowed transition. In several works it is assumed that the energy $E^{CT}(n, 3+, A)$ of the CT band is the same as $E_{Vf}(n + 1, 2+, A)$ [32, 21, 22]. However, this is not obvious and before such an assumption can be made, several aspects need to be addressed. (1) What is the initial state in the CT transition? (2) What is the final state in the CT transition? (3) What is the effect of the hole left behind on the nearest neighbour anion? (4) How does lattice relaxation affect the energy levels? (5) What is the effect of a charge compensating defect?

2.1. The initial state in the charge transfer

Suppose the initial state in the CT is any state of the valence band (see for example arrow 5 in figure 1), then the width of the valence band should contribute to the width of the charge transfer band. Figure 2 shows a histogram of the width $\Gamma^{CT}(6, 3+, A)$ of the CT band in 98 different Eu^{3+} doped compounds. The average width is 0.91 eV with a standard deviation of 0.26 eV. The width is 2–3 times larger than the typical width of fd transitions in lanthanides [33]. There are several reasons. After the charge transfer, the Eu^{3+} becomes Eu^{2+} with 18 pm larger ionic radius [34]. Unavoidably it is followed by a strong lattice relaxation leading to a large offset

Table 1. Energy $E^{CT}_{abs}(13, 3+, A)$ of CT absorption and $E^{CT}_{em}(14, 2+, A)$ of CT emission in Yb^{3+} doped compounds together with the width Γ (FWHM) at RT or lower temperature. ΔS^{CT} is the Stokes shift of CT luminescence to the $^2F_{7/2}$ ground state of Yb^{3+}. E^{so} is the energy difference between emission to the $^2F_{7/2}$ and $^2F_{5/2}$ states of Yb^{3+}. All energies are in electronvolts.

Compound	E^{CT}_{abs}	Γ^{CT}_{abs}	E^{CT}_{em}	Γ^{CT}_{em}	ΔS^{CT}	E^{so}	Ref.
YPO_4	5.96	0.68 (RT)	4.00	0.83 (RT)	1.96	1.22	[52, 53]
$LuPO_4$	6.08	0.68 (RT)	4.13	0.83 (RT)	1.95	1.17	[52]
$ScPO_4$	6.39	0.64 (10 K)	4.59	0.74 (10 K)	1.80	1.24	[29, 30]
$YAlO_3$	5.63	1.77 (9 K)	3.44	0.84 (10 K)	2.19	1.15	[30, 68]
$Y_3Al_5O_{12}$	5.79	0.66 (10 K)	3.73	0.57 (10 K)	2.06	1.19	[30, 55, 54]
$Y_3Ga_5O_{12}$	5.54	0.67 (9 K)	3.31	0.60 (9 K)	2.23	1.13	[68]
$Lu_3Al_5O_{12}$	5.99	—	3.65	0.68 (LT)	2.34	1.05	[54, 56]
$Lu_2YbAl_5O_{12}$	5.39	—	3.88		1.52	1.39	[57]
C–Y_2O_3	5.46	0.63 (10 K)	3.37	0.87 (10 K)	2.09	1.05	[30]
$LiYO_2$	5.79		3.49	—	2.30	0.99	[30]
C–Sc_2O_3	5.51		3.38	—	2.13	0.82	[30]
$NaScO_2$	5.96		3.85	—	2.11	0.97	[30]
$LiScO_2$	6.02	0.62 (10 K)	3.97	0.67 (10 K)	2.05	1.32	[30]
La_2O_2S	4.08	0.5 (80 K)	2.81	0.46 (10 K)	1.27	1.17	[58, 30]
Y_2O_2S	4.01	0.5 (80 K)	3.16	0.46 (10 K)	0.85	1.22	[58, 30]

in the configuration coordinate diagram. This may already account for the 0.91 eV width of the CT bands. Other contributions may arise when there are different lanthanide sites in the crystal or when the charge transfer brings the divalent lanthanide into one of its excited states.

The valence band can be several electronvolts wide. Therefore, when the CT would start from any level in the valence band, a much wider CT band is expected. Since this is not the case, we conclude that the initial state in the CT absorption is near or at the top of the valence band, as indicated by arrow 3 in figure 1.

Other evidence is obtained by comparing the width of the CT absorption band with the width of the CT emission band. Yb^{3+} is the only lanthanide for which CT emission is reported. A hole in the valence band created after CT relaxes rapidly to the top of that band. The CT emission is therefore surely a transition from the $^1S_0$ ground state of Yb^{2+} to the hole at the top of the valence band; see arrow 6 in figure 1. If the initial state of the CT absorption is also near the top of the valence band then the width of the CT absorption band must be almost the same as that of the CT emission band. Data available on both widths for Yb^{3+} are compiled in table 1. Considering that the error can be as large as 0.12 eV, there is indeed no significant difference. It is therefore concluded that the CT starts from the top of the valence band.

2.2. The final state in the charge transfer

In principle, the final state in the CT transition can be any of the $4f^n$ levels of the divalent lanthanide ion. In the case of Eu^{3+} and Yb^{3+} the charge transfer to excited $4f^n$ states is at much higher energy than to the $Eu^{2+}[^8S_{7/2}]$ and the $Yb^{2+}[^1S_0]$ ground states. For these lanthanides there is no uncertainty on the nature of the final state. Charge transfer to Tm^{3+} may end at the $^2F_{7/2}$ ground but also at the $^2F_{5/2}$ state at 1.08 eV higher energy; see arrow 7 in figure 1. This energy difference is still large enough to be resolved from the ground state CT band.

The energy difference with the next $4f^n$ state is about 0.6 eV for Er^{2+} and Ho^{2+}. In the case of Sm^{3+}, the final state can be any of the closely spaced levels of the $4f^6[^7F_J]$ multiplet of Sm^{2+}; see arrows 8 and 9 in figure 1. If each transition is equally probable, the charge transfer

Table 2. The energy E_{Ln}^{CT} and width Γ_{Ln}^{CT} in electronvolts of CT absorption bands of Sm^{3+}, Eu^{3+} and Yb^{3+} doped compounds. The widths are at RT unless specified otherwise.

Compound	E_{Sm}^{CT}	Γ_{Sm}^{CT}	Ref.^{Sm}	E_{Eu}^{CT}	Γ_{Eu}^{CT}	E_{Yb}^{CT}	Γ_{Yb}^{CT}	Ref.^{Yb}
CaF_2	—	—		8.18	0.64 (77 K)	8.61	0.64	[59, 40]
acetonitrile–$(LnCl_6)^{3-}$	5.34	—	[60]	4.12	—	4.55	—	[60]
$LnCl_3$	4.61	—	[25]	3.47	—	—	—	
ethanol–$LnBr_6^{3-}$	4.98	—	[24]	3.88	—	4.40	—	[24]
acetonitrile–$[LnBr_6]^{3-}$	4.34	—	[60]	3.03	—	3.63	—	[60]
$LnBr_3$	4.28	—	[25]	3.22	—	—	—	
$((C_6H_5)_3PH)_3LnI_6$	3.08	—	[38]	1.84	0.51	2.21	—	[38]
$Mg_3F_3BO_3$	5.39	0.56	[61]	4.26	0.60	—	—	
LnOCl	5.77	—	[25]	4.59	—	—	—	
YOCl	5.64	0.85	[26]	4.40	1.06	—	—	
LaOBr	5.17	—	[62]	4.03	0.78	4.66	—	[62]
LnOBr	5.51	—	[25]	4.48	—	—	—	
YOBr	5.44	—	[26]	4.29	—	—	—	
LaOI	4.77	0.74	[63]	3.70	1.20	—	—	
$CaSO_4$	5.59	1.03	[64]	4.68	0.52	—	—	
$Ln_2(SO_4)_3$	6.20	0.93	[25]	5.23	1.24	—	—	
$Sr_3(PO_4)_2$	6.11	1.23	[65]	5.41	0.99	—	—	
$LaPO_4$	6.11	0.81	[39]	4.84	0.95	5.35	0.86	[39]
$LnPO_4$	6.49	—	[25, 66]	5.34	—	—	—	
YPO_4	6.95	0.69 (6 K)	[48]	5.66	0.81	5.96	0.68	[52, 53]
$LuPO_4$	—	—		5.74	—	6.08	0.68	[52]
$ScPO_4$	—	—		6.05	—	6.39	0.64 (10 K)	[30]
$Ln_2(CO_3)_3{\cdot}3H_2O$	6.46	—	[25]	5.23	—	—	—	
$Ln_2(SO_4)_3{\cdot}8H_2O$	6.24	—	[25]	5.17	—	—	—	
$GdAl_3(BO_3)_4$	6.20	—	[26]	4.88	0.82	—	—	
$LnBO_3$	6.36	—	[66]	5.51	—	—	—	
YBO_3	—	—		5.64	1.34	5.74	—	[30]
$LuBO_3$	—	—		5.37	1.24	5.90	—	[66]
$CaBPO_5$	6.53	1.42	[67]	5.06	1.05	—		
$LaAlO_3$	5.17	—	[26]	4.00	1.09	5.08	—	[30]
$GdAlO_3$	5.77	—	[26]	4.73	0.40 (80 K)	—	—	
$Y_3Al_5O_{12}$	—	—		5.54	—	5.79	0.66 (10 K)	[30, 55]
$Y_3Ga_5O_{12}$	—	—		5.28	—	5.54	0.67 (9 K)	[68]
$NaLaO_2$	—	—		4.58	—	4.73	—	[30]
$LiLaO_2$	—	—		4.53	—	4.92	—	[30]
$SrLa_2BeO_5$	5.06	—	[70]	3.88	0.61 (10 K)	—	—	
C–Y_2O_3	—	—		5.06	0.93	5.46	0.63 (10 K)	[30]
$LiYO_2$	—	—		5.17	1.18	5.79	—	[30]
$NaScO_2$	—	—		5.51	—	5.96	—	[30]
$LiScO_2$	—	—		5.56	—	6.02	0.62 (10 K)	[30]
La_2O_2S	4.64	0.62	[39]	3.57	—	4.08	0.5 (80 K)	[58, 30]
Y_2O_2S	4.79	0.62	[39]	3.60	0.52	4.01	—	[30, 58]
CaS	3.54	—	[71]	2.21	—	—	—	

band of Sm^{3+} broadens by ≈0.5 eV on top of the normal width of 0.9 eV. Furthermore the CT band shifts 0.2–0.3 eV towards higher energy.

Data on the width of the CT bands of Sm^{3+}, presented in table 2, do not reveal a systematically larger width than of Eu^{3+} or Yb^{3+}. In particular, the results for Sm^{3+}, Eu^{3+}, Tm^{3+}, and Yb^{3+} in YPO_4, which are the most reliable data available [48, 45], do not indicate

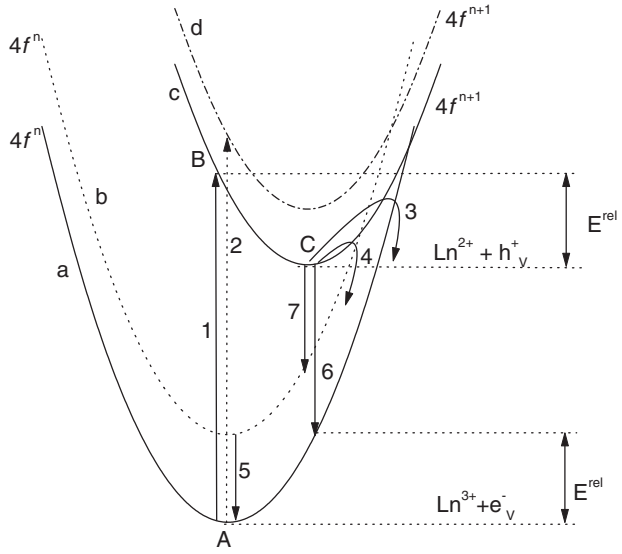

Figure 3. Configuration coordinate diagram illustrating the transitions and lattice relaxation involved in charge transfer absorption and luminescence.

a significant difference. For these lanthanides the CT band width is on average 0.70 ± 0.06. Apparently the oscillator strength for the charge transfer to the $^7F_0$ ground state of Sm^{2+} is much larger than that for the transfer to the higher $^7F_{J=1-6}$ levels. We therefore assume in the rest of this work that the final state in the CT is the ground state of the divalent lanthanide.

2.3. Lattice relaxation and electron–hole binding

One may view the charge transfer as a local transition from an anion to the lanthanide [35]. This is illustrated by the configuration coordinate diagram in figure 3. Initially the system is at point A on parabola (a) corresponding with an electron at the top of the valence band (e_V^-) and a Ln^{3+} ion. The CT to the ground state (arrow 1) of the divalent lanthanide is more probable than that to an excited state (arrow 2). The divalent lanthanide has ≈18 pm larger ionic radius than the original trivalent one, and the system relaxes strongly and moves to point C.

From here several routes can be followed.

(1) Intersystem crossing back to parabola (a) (arrow 3) and all luminescence is quenched.
(2) Intersystem crossing to an excited state of Ln^{3+} (arrow 4 and parabola (b)). This is a common situation for Eu^{3+} and it leads to narrow band 4f → 4f emission (arrow 5).
(3) A luminescence transition to the ground state (arrow 6) or an excited 4f state (arrow 7) of Ln^{3+}.

This latter situation occurs in Yb^{3+}. In addition to the charge transfer emission to the $^2F_{7/2}$ state, emission to the $^2F_{5/2}$ excited state also occurs. The energy difference E^{so} between both luminescence bands is compiled in table 1. On average it appears 0.07 eV smaller than the spin–orbit splitting of 1.24 eV observed under direct $^2F_{7/2} \rightarrow {}^2F_{5/2}$ excitation. Furthermore, there is a rather wide spread in the values. It may be caused by a slight shift of parabola (b) relative to parabola (a) or it may indicate non-harmonic behaviour when the configuration coordinate offset is large.

The relaxation involved in the CT process leads to large Stokes shift ΔS^{CT} between emission and absorption. The values available for Yb^{3+} are compiled in table 1. Apart from $Y_3Ga_5O_{12}$, $Lu_3Al_5O_{12}$, and Y_2O_2S all compounds have a Stokes shift around 1.95 ± 0.25 eV. This is more than two times larger than the average width of the CT emission and CT absorption bands. Usually, like for df emission, Stokes shift and width are of comparable magnitude [42]. Probably some sort of self-trapping of the hole component into for example a V_k-like centre takes place after the charge transfer. Ion displacements other than that in the harmonic model of the configuration coordinate diagram are involved in this self-trapping [36]. In that case the self-trapping energy adds to the Stokes shift.

Since CT ends at point B in figure 3, the CT energy overestimates the energy difference E_{Vf} between the top of the valence band and the $4f^n$ ground state by the relaxation energy E^{rel}. When the configuration coordinate diagram applies to our situation then $E^{rel} = 0.5 \times \Delta S \approx$ 0.5–1.0 eV. On the other hand the Coulomb attraction between the hole on the anion and the transferred electron reduces the CT energy. Fortuitously, this energy is also of the order 0.5–1.0 eV and it cancels to a large extent E^{rel}.

Putting everything together, we arrive at a situation where $E_{Vf}(n + 1, 2+, A) \approx E^{CT}(n, 3+, A)$, and one may write

$$E_{VC}(A) = E^{CT}(n, 3+, A) + E_{fd}(n + 1, 2+, A) + E_{dC}(n + 1, 2+, A) \tag{2}$$

where $E_{VC}(A)$ is the energy difference between the top of the valence band (V) and the bottom of the conduction band (C). Actually $E_{VC}(A)$ is defined as the threshold energy needed to create a free electron in the conduction band by means of optical excitation. This energy is larger than the fundamental absorption onset $E^{fa}(A)$ of the host lattice by an amount equal to the exciton binding energy.

Equation (2) can also be written as

$$E_{VC}(A) = E^{CT}(n, 3+, A) + E^{pc}(n + 1, 2+, A) \tag{3}$$

where E^{pc} is the photoconductivity threshold, i.e., the threshold needed to excite an electron from the $4f^n$ ground state of the divalent lanthanide to the bottom of the conduction band.

Equation (3) is known as the Born–Haber cycle and has been applied several times to locate impurity energy levels [21, 22, 32, 16]. The validity of equation (3) arises from the fortuitous circumstance that the electron–hole binding E_b^{eh} in the final state of CT compensates for E^{rel}. At this moment it is not known to what extend both energies cancel out and how it depends on the type of compound (fluorides, chlorides, bromides, iodides, oxides, sulfides).

2.4. The role of charge compensating defects

Suppose a trivalent lanthanide is on a divalent cation site with a nearby charge-compensating defect. After the charge transfer, the compensating centre is still present that would not have been there when the divalent cation site was initially occupied by a divalent lanthanide. Even with cancellation of E_b^{eh} against E^{rel}, one may question whether the CT energy provides a good measure of the location of the $4f^n$ ground state. Radzhabov [16] notes that in several oxides the right-hand side of equation (3) is 0.5 eV smaller than E_{VC}, and in halide crystal they found deviations of 1–3 eV. By systematically studying the CT bands in as wide range of compounds possible and testing the equality in equations (2) and (3), it is expected that the errors made can be determined.

Table 3. The energy E^{CT}_{Ln} in electronvolts of CT absorption bands of trivalent lanthanides in compounds.

Compound	E^{CT}_{Sm}	E^{CT}_{Eu}	E^{CT}_{Dy}	E^{CT}_{Er}	E^{CT}_{Tm}	Ref.
$LiCaAlF_6$	—	8.08	—	—	10.00	[69]
$LaCl_3$	4.49	—	5.28	5.60	—	[72, 73]
$LnBr_6^{3-}$–ethanol	4.98	3.88	—	—	5.51	[24]
acetonitrile–$[LnBr_6]^{3-}$	4.34	3.03	—	—	4.77	[60]
$((C_6H_5)_3PH)_3LnI_6$	3.08	1.84	—	—	3.48	[38]
$LaF_3:O^{2-}$	—	4.86	6.88	6.97	—	[74, 27, 75]
$YF_3:O^{2-}$	—	5.17	7.09	7.52	—	[27]
LaOBr	5.17	3.99	—	—	5.59	[76, 62]
LaOI	4.77	3.70	—	—	5.17	[63]
$LaPO_4$	6.11	4.84	7.08	7.17	6.63	[39]
YPO_4	6.93	5.66	7.65	—	7.25	[48]
$CaGa_2S_4$	3.07				3.29	[77, 78]

3. Data on charge transfer energies

The charge transfer bands are observed as 0.6–1.2 eV broad and intense bands in absorption, reflection, and excitation spectra. They have been extensively studied in the literature of the past 40 years, mostly from an application point of view. This literature was collected and reanalysed to obtain information on the CT energy of the trivalent lanthanides in about 200 different compounds. Most information is on Eu^{3+} and that will be presented elsewhere [37]. The interest of the present work is to compare the CT energy of one lanthanide in a compound with that of another lanthanide in the same compound. Therefore, data are presented on those compounds where information on the CT energy of at least two different lanthanides is available.

The data on the energy of the CT band maximum of Sm^{3+}, Eu^{3+}, and Yb^{3+} are compiled in table 2. When it could be determined, the width of the CT absorption, reflection, or excitation band is given. References to the original literature from where the Eu^{3+} data were obtained will be presented elsewhere [37]. In the compilation data on pure lanthanide compounds like $LnCl_3$ and LnOCl and lanthanide complexes in solution like acetonitrile–$(LnCl_6)^{3-}$, ethanol–$LnBr_6^{3-}$ are also included. $((C_6H_5)_3PH)_3LnI_6$ is an organic compound with ionic LnI_6^{3-} complexes [38].

In table 3 sparse data on other lanthanides are compiled. There is no information available on the CT to La^{3+}, Ce^{3+}, Pr^{3+}, Nd^{3+}, Pm^{3+}, Gd^{3+}, Tb^{3+}, and Ho^{3+}. Often the CT band is at too high energy and obscured by either host lattice or fd absorption bands. The data on $LaF_3:O^{2-}$ and $YF_3:O^{2-}$ are from trivalent lanthanides on sites with an O^{2-} impurity anion in the first anion coordination sphere.

Figure 4 shows the energy $E^{CT}(n, 3+, A)$ of the charge transfer band in Yb^{3+} ($n = 13$), Eu^{3+} ($n = 6$), and Sm^{3+} ($n = 5$), against that of Eu^{3+}. The data on Sm, and Yb fall along sets of lines parallel to that for Eu. This means that, independent of the type of compound, there is always a fixed energy difference between the CT bands of these lanthanides. The scatter in data falls usually within the accuracy of ± 0.12 eV in the CT band energies. Significant deviations are for Yb^{3+} in $LaAlO_3$, $NaLaO_3$, and YBO_3 and for Sm^{3+} in $Sr_3(PO_4)_2$. Probably the data are incorrect and they will be disregarded in further analysis. The sparse data on Tm^{3+}, Er^{3+} and Dy^{3+} in table 3 are displayed in figure 5. Here again fixed energy differences with data on Eu^{3+} and Sm^{3+} are observed.

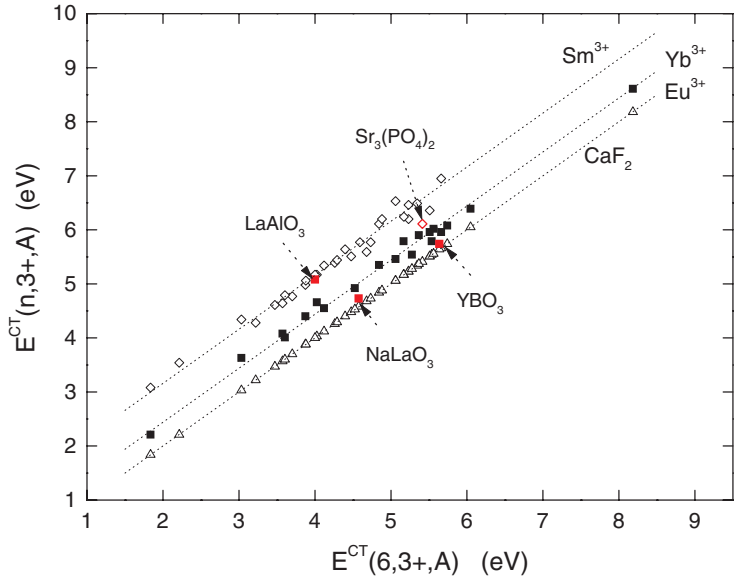

Figure 4. The energy of the charge transfer absorption band $E^{CT}(n, 3+, A)$ of Sm^{3+}, Eu^{3+}, and Yb^{3+} in compounds against that of Eu^{3+}.

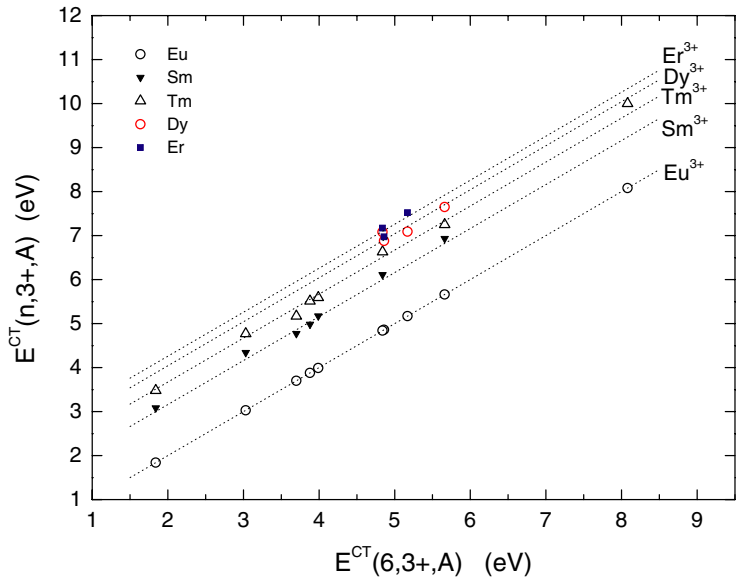

Figure 5. The energy of the charge transfer absorption band $E^{CT}(n, 3+, A)$ of Sm^{3+}, Eu^{3+}, Dy^{3+}, Er^{3+}, and Tm^{3+} in compounds against that of Eu^{3+}.

4. Discussion

The fixed difference between the energy of CT to a trivalent lanthanide ion with that to Eu^{3+} can be exploited to locate the ground state of the divalent lanthanide ion. One may use

$$E_{Vf}(n+1, 2+, A) \approx E^{CT}(n, 3+, A) = E^{CT}(6, 3+, A) + \Delta E^{CT}(n, 6, 3+) \quad (4)$$

Table 4. Energy differences $\Delta E^{CT}(n, 6, 3+)$ with Eu^{3+} CT band energies. The number in brackets in column 3 is the number of compounds used in averaging. $E_{Afree}(n+1, 2+)$ and $\Delta E_{Vd}^{calc}(n+1, 2+)$ are from [19]. n is the number of electrons in the $4f^n$ configuration of the trivalent lanthanide. All energies are in electronvolts.

Ln^{3+}	n	ΔE^{CT} $(n, 6, 3+)$	E_{Afree} $(n+1, 2+)$	ΔE_{Vd} $(n+1, 7, 2+)$	ΔE_{Vd}^{calc} $(n+1, 7, 2+)$	ΔE_{Vd} $(n+1, 7, 2+)$	ΔE_{Vf} $(n+1, 7, 2+)$
La	0		−0.94	—	0.04	0.04	5.19
Ce	1		0.35	—	0.01	0.00	3.87
Pr	2	2.44 (1)	1.56	−0.22	−0.01	−0.01	2.65
Nd	3	2.29 (1)	1.93	0.00	−0.02	−0.02	2.27
Pm	4		1.96	—	−0.02	−0.01	2.24
Sm	5	1.16 (29)	3.00	−0.06	−0.01	−0.01	1.21
Eu	6	0	4.22	0.00	0	0	0
Gd	7	—	−0.10	—	0	0	4.32
Tb	8	—	1.19	—	0.12	0.10	3.12
Dy	9	2.04 (4)	2.12	−0.06	0.23	0.19	2.28
Ho	10	2.42 (1)	2.25	0.45	0.32	0.26	2.23
Er	11	2.26 (3)	2.12	0.16	0.40	0.33	2.43
Tm	12	1.67 (8)	2.95	0.40	0.49	0.40	1.67
Yb	13	0.44 (20)	4.22	0.44	0.57	0.47	0.47

where the CT energy of Eu^{3+} is used as a common reference. $\Delta E^{CT}(n, 6, 3+) \equiv \overline{E^{CT}(n, 3+, A) - E^{CT}(6, 3+, A)}$ is the difference between the energy of CT to the trivalent lanthanide with that to Eu^{3+} averaged over all compounds A for which data are available.

The values for $\Delta E^{CT}(n, 6, 3+)$ together with the number of compounds used in averaging are compiled in column 3 of table 4. Values are most reliable for Sm^{3+}, Tm^{3+}, and Yb^{3+}. The information on $E^{CT}(n, 6, 3+)$ for $n < 5$ is very scarce. In data by van Pieterson *et al* [41] on YPO_4:Nd^{3+}, a band is observed near 156 nm that was attributed to fd excitation in Nd^{3+}. However, it can also be the CT band of Nd^{3+} providing the value for $E^{CT}(3, 6, 3+) = 2.29$ eV in table 4. In the absorption spectrum and the excitation spectrum of CaF_2:Pr^{3+}, a broad band is seen that overlaps with the fundamental absorption onset at 10.6 eV [40, 41]. When we attribute this band to the CT transition it provides $E^{CT}(2, 6, 3+) = 2.44$ eV in table 4. A broad feature around 171 nm in the reflection spectrum of $LaPO_4$:Ho^{3+} was ascribed to CT, and it provides $E^{CT}(10, 6, 3+) = 2.42$ eV [39].

Combining equation (4) with equation (1) one may position the first 5d level above the top of the valence band

$$E_{Vd}(n+1, 2+, A) = E^{CT}(6, 3+, A) + \Delta E^{CT}(n, 6, 3+) + E_{Afree}(n+1, 2+) - D(2+, A) \qquad (5)$$

where the values of $E_{Afree}(n+1, 2+)$ are given in table 4 [20].

The energy difference between the first 5d level of a divalent lanthanide and that of Eu^{2+} is given by

$$\Delta E_{Vd}(n+1, 7, 2+) \equiv \overline{E_{Vd}(n+1, 2+, A) - E_{Vd}(7, 2+, A)}$$
$$= \Delta E^{CT}(n, 6, 3+) + E_{Afree}(n+1, 2+) - E_{Afree}(7, 2+). \qquad (6)$$

The values are compiled in column 5 of table 4 and shown in figure 6. The errors in the data on Sm, Dy, Er, Tm, and Yb are from the standard deviation in $\Delta E^{CT}(n, 6, 3+)$. Within 0.7 eV for each divalent lanthanide the energy of the lowest 5d level is constant. Nevertheless, those of Tm^{2+} and Yb^{2+} are always significantly (0.46 eV) higher than those of Sm^{2+} and Eu^{2+}. This result is in excellent agreement with results from a study on anomalous divalent lanthanide emission [19]. It was found that the autoionization threshold $E_{dC}(14, 2+, A)$ for Yb^{2+} is always

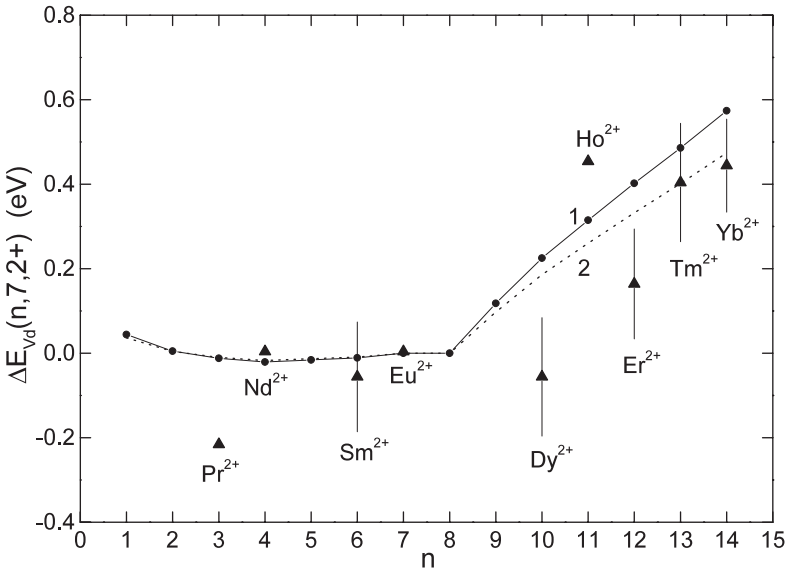

Figure 6. ΔE_{Vd} values for divalent lanthanides determined from charge transfer energies. Curve 1: semi-empirically calculated values from [19]. Curve 2: adopted values in this work.

smaller than $E_{\mathrm{dC}}(7, 2+, A)$ of Eu^{2+} leading to higher probability for anomalous emission in Yb^{2+} doped compounds. This was explained by the combined effect of

(1) the Coulomb attraction between the 5d electron and the lanthanide ion,
(2) the isotropic exchange interaction between the 5d electron spin and the total spin of the $n - 1$ electrons in the 4f core, and
(3) a correction to the Coulomb interaction and electron–electron repulsion at the lanthanide site due to lattice relaxation.

Column 6 of table 4 and curve 1 in figure 6 show the values for $\Delta E_{\mathrm{Vd}}(n + 1, 7, 2+)$ that were calculated semi-empirically in [19] from the above three effects. It predicted an almost constant 5d level energy for the lanthanides with $n + 1 < 8$, and a gradual increase by 0.57 eV from Eu^{2+} to Yb^{2+}. The data on CT energies of Eu^{2+}, Sm^{2+}, Tm^{2+} and Yb^{2+} agree very well with this trend. Since the 5d energy in Yb^{2+} and Tm^{2+} is on average 20% smaller than suggested with the semi-empirical model, column 7 and curve 2 in figure 6 show $\Delta E_{\mathrm{Vd}}(n + 1, 7, 2+)$ corrected for this 20%. The data on Dy^{2+} still appear 0.3 eV too low. This may be related to an underestimation of the value for $E_{A\mathrm{free}}(10, 2+)$ in [20]. From now on the corrected values for $\Delta E_{\mathrm{Vd}}(n + 1, 7, 2+)$ are regarded as the most likely trend in the lowest 5d level position of divalent lanthanides in compounds as a function of n. Using these values and equation (6), the values of $\Delta E_{\mathrm{Vf}}(n, 6, 3+)$ in column 8 are obtained. These values will be regarded as the most likely trend in the location of the lowest $4f^{n+1}5d^0$ level.

With equations (4), (5), and the values for $\Delta E_{\mathrm{Vf}}(n + 1, 7, 2+)$ and $E_{A\mathrm{free}}(n + 1, 2+)$ it is possible to draw the impurity levels of the divalent lanthanides relative to the conduction and valence band of the host crystal. The only additional compound dependent information needed are: (1) the CT band energy $E(6, 3+, A)$ of Eu^{3+}, (2) the redshift $D(2+, A)$, and (3) the band gap $E_{\mathrm{VC}}(A)$.

Literature provides values for $E^{\mathrm{CT}}(6, 3+, A)$ in about 200 different compounds. These data are presented in a forthcoming paper together with values of $E_{\mathrm{VC}}(A)$ [37]. Values of

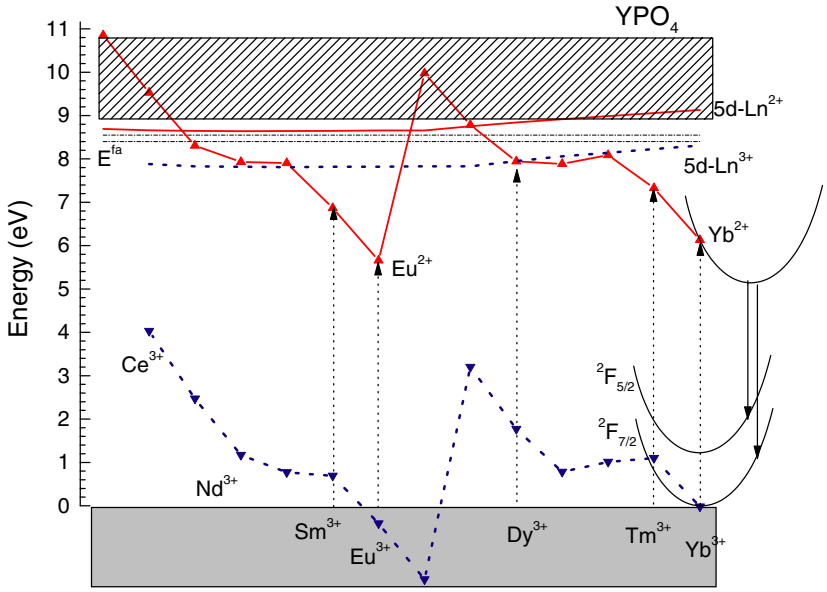

Figure 7. Energy level schemes of divalent and trivalent lanthanides in YPO_4. The dashed arrows indicate charge transfer energies to the trivalent lanthanides. The solid arrows for Yb^{2+} indicate the charge transfer emissions in a configuration coordinate scheme.

$D(2+, A)$ for more than 300 compounds have already been presented in [42]. The redshift $D(2+, A)$ is usually not available for divalent lanthanides on trivalent lattice sites, but a good estimate can be made from the relationship [43]

$$D(2+, A) = 0.64D(3+, A) - 0.233\ \text{eV} \tag{7}$$

where $D(3+, A)$ is the redshift in trivalent lanthanides. Therefore the compilation on $D(3+, A)$ values on 300 different compounds can also be used [33].

4.1. Application of the three-parameter model

We first apply the method to YPO_4. $D(3+, YPO_4) = 2.20$ eV [33], and the onset of the fundamental absorption in YPO_4 is found at $E^{fa} = 8.0$ eV at room temperature (RT) and at 8.4 eV at 10 K [44, 45]. The maximum of the phosphate group excitation is at slightly higher energy of $E^{ex} = 8.2$ eV (RT) and 8.55 eV (10 K). The bottom of the conduction band is defined as the threshold energy where free electrons and free holes are created. One may question whether this already occurs when the phosphate group is excited. The bottom of the conduction band formed from Y states is estimated somewhat higher at $E_{VC} = 9.0 \pm 0.2$ eV.

Figure 7 shows the level scheme constructed by using equations (4) and (5) where instead of ΔE^{CT} the values for ΔE_{Vf} in table 4 were used. The horizontal dashed lines are at energies E^{fa} and E^{ex}. The dashed arrows starting from the top of the valence band, defined as the zero point of energy, indicate the observed CT transitions to Sm^{3+}, Eu^{3+}, Dy^{3+}, Tm^{3+}, and Yb^{3+}. For Yb, the CT emission transitions leaving Yb^{3+} in the $^2F_{7/2}$ or $^2F_{5/2}$ state together with the configuration coordinate diagram are also shown; see also figure 3.

For each divalent lanthanide ion the 5d level is located very close to the bottom of the conduction band of YPO_4. This means that the 5d state is not stable against autoionization.

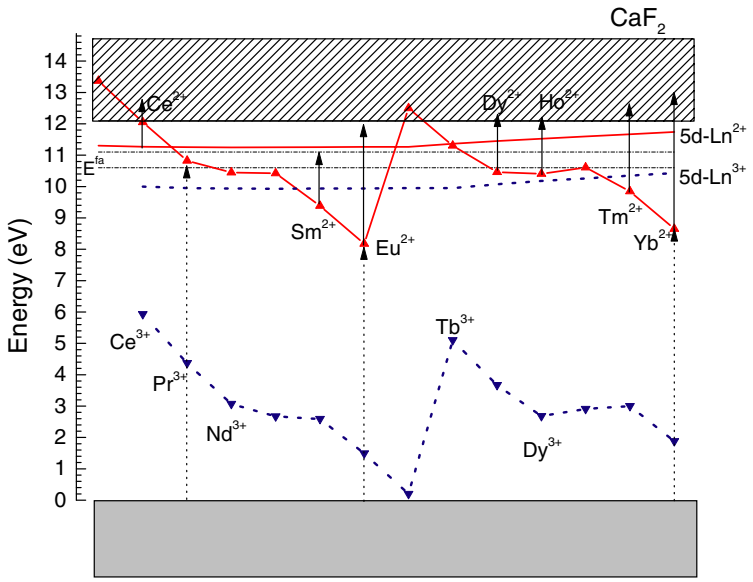

Figure 8. Energy level schemes of divalent and trivalent lanthanides in CaF_2. The dashed arrows indicate charge transfer energies to the trivalent lanthanides. The solid arrows indicate threshold energies from photoconductivity experiments.

This is consistent with the fact that df emission is never observed for divalent lanthanides on trivalent lattice sites [42].

Applying the method to CaF_2 provides the level scheme shown in figure 8. The same E^{fa}, E^{ex}, and E_{VC} values as in [19] were used. The three dashed arrows indicate observed CT transitions (that of Pr is still tentative). The solid arrows indicate observed photoionization thresholds [19]. According to the Born–Haber cycle of equation (3) they should end at the bottom of the conduction band. This appears indeed the case for Eu, Dy, and Ho, but there are significant deviations for Ce, Tm, and Yb. Possible reasons have been discussed elsewhere [19].

Contrary to the situation in YPO_4, the first $4f^{n-1}5d$ level for each lanthanide is located well below the bottom of the conduction band. $E_{dC}(7, 2+, CaF_2)$ is large enough for normal df emission in Eu^{2+}. The 0.46 eV smaller value for $E_{dC}(14, 2+, CaF_2)$ brings the 5d state of Yb^{2+} close to the conduction band and anomalous emission involving conduction band states is observed [46, 19].

It is easy to modify equations (4) and (5) for the energy levels of the trivalent lanthanides by using information on the CT to tetravalent lanthanides. However, there is too little information available on such transitions. Instead we will make the following assumption:

$$\Delta E_{Vd}(n, 1, 3+) = 1.2 \times (\Delta E_{Vd}(n, 7, 2+) - \Delta E_{Vd}(1, 7, 2+)). \quad (8)$$

The factor 1.2 is introduced to take into account that the exchange interaction between the 5d electron and $4f^n$ electrons, the Coulomb interaction between 5d and the lanthanide, and the corrections due to lattice relaxation are estimated to be 20% larger in the smaller trivalent lanthanides [47, 19]. Ce^{3+} ($n = 1$) is used as the reference trivalent lanthanide ion instead of Eu^{2+} ($n = 7$) for the divalent lanthanides.

The values for $\Delta E_{Vd}(n, 1, 3+)$ are in table 5. With $E_{Afree}(n, 3+)$ for trivalent lanthanides from [31, 47], the $\Delta E_{Vf}(n, 1, 3+)$ are obtained; see table 5. One only needs to establish the location of the first 5d or the 4f level of Ce^{3+} to generate the level positions for each trivalent lanthanide.

Table 5. Host independent parameters needed to draw the lowest 5d or the lowest 4f levels of the trivalent lanthanides relative to the bands of the host lattice. $E_{Afree}(n, 3+)$ are from [31, 47]. n is the number of electrons in the $4f^n$ configuration of the trivalent lanthanide. All energies are in electronvolts.

Ln^{3+}	n	$\Delta E_{Vd}(n, 1, 3+)$	$E_{Afree}(n, 3+)$	ΔE_{Vf} (n,1,3+)
Ce	1	0	6.12	0
Pr	2	−0.05	7.63	−1.56
Nd	3	−0.06	8.92	−2.86
Pm	4	−0.07	9.31	−3.26
Sm	5	−0.06	9.40	−3.34
Eu	6	−0.06	10.5	−4.44
Gd	7	−0.05	11.8	−5.73
Tb	8	−0.05	6.90	−0.83
Dy	9	0.07	8.45	−2.26
Ho	10	0.18	9.55	−3.25
Er	11	0.26	9.40	−3.02
Tm	12	0.35	9.40	−2.93
Yb	13	0.43	10.6	−4.05
Lu	14	0.52	12.0	−5.36

In the case of CaF_2 a fair estimate can be given for the location of the $5d_e$ and $5d_t$ levels of Ce^{3+}. The absence of vibronic structure in the $4f \rightarrow 5d_t$ excitation band of Ce^{3+} in CaF_2 is ascribed to a very short lifetime of the $5d_t$ state due to a rapid autoionization process [48]. Therefore, the $5d_t$ state is inside the conduction band. For figure 8, we assumed that it is located just above the bottom of the conduction band at 12.4 eV. The $5d_e$ level at 2.59 eV lower energy provides then $E_{Vd}(1, 3+, CaF_2) = 9.81$ eV, and from that level energies for each trivalent lanthanide ion in CaF_2 are obtained; see figure 8.

The same procedure can be followed for YPO_4. The absence of vibronic structure in the second 5d band at 1.12 eV above the first 5d band locates the second band inside the conduction band [48]. We have assumed a position at the bottom of the conduction band and from that all level positions of the trivalent lanthanides were generated; see figure 7. In CaF_2 and YPO_4, the first 5d level of the trivalent lanthanide is 1.2 and 0.8 eV, respectively, below the first 5d level of the corresponding divalent lanthanide. This must be attributed to the larger Coulomb binding of the 5d electron in the higher charged trivalent lanthanide ion.

Schemes like those for YPO_4 and CaF_2 can be constructed in principle for each compound with few parameters. They are very valuable in understanding the mechanisms involving luminescence and charge trapping and helpful in the interpretation of spectra. It is immediately clear that Ce^{3+}, Pr^{3+}, and Tb^{3+} are stable hole traps in YPO_4. Nd^{3+} provides a more shallow hole trap. Sm^{3+}, Eu^{3+}, and Yb^{3+} provide stable and deep electron traps because the ground state of the divalent lanthanides is well below the conduction band edge. Nd^{3+}, Dy^{3+}, Ho^{3+} and Er^{3+} are relatively shallow electron traps.

In the search for persistent afterglow materials a charge trap shallow enough to allow for a slow release of the trapped charges at RT is a prerequisite. The observation that Nd^{3+} and Dy^{3+} enhance the persistent afterglow in aluminates like $CaAl_2O_4$ and $SrAl_2O_4$ and that Sm^{3+} and Yb^{3+} suppress the afterglow is linked directly to the depth of electron traps [7]. The deep trap in Sm^{3+} can be utilized for storing information as in storage phosphors and optical memories [8, 9, 49].

The schemes are also crucial for understanding luminescence quenching mechanisms. Quenching via autoionization to conduction band levels was already discussed in [19]. Thermal

excitation to conduction band levels is an important quenching mechanism for Ce^{3+} df emission [1, 2]. It is known that in Ce^{3+} and Eu^{3+} co-doped systems mutual quenching of Ce and Eu luminescence is a general phenomenon [50]. Figures 7 and 8 reveal that the 5d state of Ce^{3+} is located above the ground state of Eu^{2+} enabling electron transfer to Eu^{3+} after excitation of the Ce^{3+} 5d level. Backtransfer from Eu^{2+} to Ce^{4+} then completes the quenching route of Ce^{3+} df emission. In LaB_3O_6:Ce^{3+} doped with Eu^{3+}, the Eu^{3+} CT band coincides with the fd band of Ce^{3+} also resulting in such mutual quenching [51]. These examples illustrate the importance of schemes where the lowest 4f and 5d levels of both divalent and trivalent lanthanides are drawn relative to conduction and valence band of the host crystal.

In [19] it was found that the probability for anomalous emission is larger for Yb^{2+} than for Eu^{2+}, which is an immediate consequence of the 0.5 eV higher energy of the 5d state.

Impurity level schemes based on CT band energies are subject to a possible systematic error of 0.5 eV. Similar errors exist when information on photoconductivity thresholds, or UPS and XPS data, are used [12, 13]. Furthermore the bottom of the conduction band usually raises by several tenths of an electronvolt when the temperature is lowered from 300 to 10 K. The presence or absence of charge compensating defects may also change electron energy levels, typically by 0.5 eV. Clearly at the 0.5 eV scale there are still many uncertainties on the absolute level positions. However, most of the error is systematic with n. When $E_{dC}(n, 2+, A)$ is smaller than 1 eV such systematic uncertainty can be of crucial importance for the final performance of the material.

Combining the results in this work with other information on impurity level positions may reveal these errors and allow for a more detailed description of level positions. For example,

(1) the presence or absence of anomalous emission in divalent lanthanides,
(2) the quenching of df emission due to autoionization or thermal excitation to conduction band levels,
(3) photo-conductivity studies,
(4) ultra violet and XPS, and
(5) the presence or absence of vibronics in higher lying 5d levels of Ce^{3+},

all provide such additional information.

5. Summary and conclusions

The systematic variation in the transfer of an electron from the valence band to a trivalent lanthanide in compounds was studied. It was found that

(1) the width of the CT band in spectra does not correlate with the width of the valence band,
(2) the width of the CT luminescence in Yb^{3+}-doped compounds is about the same as the width of the CT absorption, and
(3) there is no significant dependence of the width of CT band on type of lanthanide.

From these observations, it was concluded that the CT starts from the top of the valence band and ends in the ground state of the divalent lanthanide.

It was estimated that the CT band energy overestimates the energy E_{Vf} of the 4f ground state by $\approx$0.5–1.0 eV because of the relaxation that follows the CT. It was also estimated that the CT band energy underestimates E_{Vf} by 0.5–1.0 eV because of the residual Coulomb interaction with the hole left behind. This tends to cancel out the relaxation effect, and then the CT energy provides a good measure of E_{Vf}. The error is assumed to be systematic for each lanthanide and of the order of 0.5 eV.

By comparing the CT energies for different trivalent lanthanides in the same host, constant energy differences that are compiled in table 4 were revealed. This provides large predictive potential. For example, once the CT band is known for Eu^{3+} that of others can be predicted. Combining the systematic variation in the CT band energies with the systematic variation in fd transition energies, the $4f^n$ and $4f^{n-1}5d$ levels of each divalent lanthanide ion can be drawn relative to the bottom of the conduction band and the top of the valence band. Three additional compound dependent parameters are needed: (1) the charge transfer energy $E^{CT}(6, 3+, A)$ of Eu^{3+}, (2) the redshift $D(2+, A)$, and (3) the location of the bottom of the conduction band $E_{VC}(A)$.

Whereas the energy of the lowest $4f^n$ state varies by 6 eV through the lanthanide series, the lowest $4f^{n-1}5d$ energy is remarkably constant. It appears that the 5d state of Yb^{2+} and Tm^{2+} is always about 0.5 eV closer to the conduction band than that of Eu^{2+} and Sm^{2+}. This agrees with results and observations on anomalous luminescence in the divalent lanthanides.

With similar methods as used for divalent lanthanides the level positions of trivalent lanthanides can also be found. YPO_4 and CaF_2 were used as examples. A complete picture of divalent and trivalent lanthanide impurity levels in compounds is obtained that is very useful to understand and predict aspects concerning luminescence, luminescence quenching, anomalous luminescence, ESA, charge trapping, persistent afterglow, storage properties, and scintillation mechanisms.

References

[1] Blasse G, Schipper W and Hamelink J J 1991 *Inorg. Chim. Acta* **189** 77
[2] Lyu L-J and Hamilton D S 1991 *J. Lumin.* **48/49** 251
[3] Cheung Y M and Gayen S K 1994 *Phys. Rev.* B **49** 14827
[4] Hamilton D S, Gayen S K, Pogatshnik G J, Ghen R D and Miniscalco W J 1989 *Phys. Rev.* B **39** 8807
[5] Pedrini C, Bouttet D, Dujardin C, Belsky A and Vasil'ev A 1996 *Proc. Int. Conf. on Inorganic Scintillators and Their Applications* ed P Dorenbos and C W E van Eijk (The Netherlands: Delft University Press) p 103
[6] Matsuzawa T, Aoki Y, Takeuchi N and Murayama Y 1996 *J. Electrochem. Soc.* **143** 2670
[7] Hölsa J, Junger H, Lastusaari M and Niittykoski J 2001 *J. Alloys Compounds* **323/324** 326
[8] Meijerink A, Schipper W J and Blasse G 1991 *J. Phys. D: Appl. Phys.* **24** 997
[9] Chakrabarti K, Mathur V K, Rhodes J F and Abbundi R J 1988 *J. Appl. Phys.* **64** 1363
[10] Nanto H, Douguchi Y, Nishishita J-I, Kadota M, Kashiwagi N, Shinkawa T and Nasu S 1997 *Japan. J. Appl. Phys.* **36** 421
[11] Sato S 1976 *J. Phys. Soc. Japan* **41** 913
[12] Thiel C W, Gruguel H, Wu H, Sun Y, Lapeyre G J, Cone R L, Equall R W and Macfarlane R M 2001 *Phys. Rev.* B **64** 085107
[13] Thiel C W, Gruguel H, Sun Y, Lapeyre G J, Macfarlane R M, Equall R W and Cone R L 2001 *J. Lumin.* **94/95** 1
[14] Thiel C W, Sun Y and Cone R L 2002 *J. Mod. Opt.* **49** 2399
[15] Pedrini C, Rogemond F and McClure D S 1986 *J. Appl. Phys.* **59** 1196
[16] Radzhabov E 2001 *J. Phys.: Condens. Matter* **13** 10955
[17] Lawson J K and Payne S A 1991 *J. Opt. Soc. Am.* B **8** 1404
[18] McClure D S and Pedrini C 1985 *Phys. Rev.* B **32** 8465
[19] Dorenbos P 2003 *J. Phys.: Condens. Matter* **15** 2645
[20] Dorenbos P 2003 *J. Phys.: Condens. Matter* **15** 575
[21] Happek U, Basun S A, Choi J, Krebs J K and Raukas M 2000 *J. Alloys Compounds* **303** 198
[22] Happek U, Choi J and Srivastava A M 2001 *J. Lumin.* **94/95** 7
[23] McClure D S, Wong W C and Basun S A 1995 *Radiat. Eff. Defects Solids* **135** 27
[24] Jörgensen C K 1962 *Mol. Phys.* **5** 271
[25] Barnes J C and Pincott H 1966 *J. Chem. Soc.* a 842
[26] Blasse G and Bril A 1966 *Phys. Lett.* **23** 440
[27] Gerard I, Krupa J C, Simoni E and Martin P 1994 *J. Alloys Compounds* **207/208** 120
[28] Krupa J C 1995 *J. Alloys Compounds* **225** 1

[29] van Pieterson L and Meijerink A 2000 *J. Alloys Compounds* **300** 426
[30] van Pieterson L, Heeroma M, de Heer E and Meijerink A 2000 *J. Lumin.* **91** 177
[31] Dorenbos P 2000 *J. Lumin.* **91** 91
[32] Wong W C, McClure D S, Basun S A and Kokta M R 1995 *Phys. Rev.* B **51** 5682
[33] Dorenbos P 2000 *J. Lumin.* **91** 155
[34] Shannon R D 1976 *Acta Crystallogr.* A **32** 751
[35] Hoshina T, Imanaga S and Yokono S 1977 *J. Lumin.* **15** 455
[36] Song K S and Williams R T 1993 *Self-Trapped Excitons* (*Springer Series in Solid State Sciences* vol 105) (Berlin: Springer)
[37] Dorenbos P 2003 at press
[38] Ryan J L 1969 *Inorg. Chem.* **8** 2053
[39] Nakazawa E and Shiga F 2003 *Japan. J. Appl. Phys.* **42** 1642
[40] Szczurek T and Schlesinger M 1985 Rare earths spectroscopy *Proc. Int. Symp. on Rare Earths Spectroscopy (Wroclav, Poland, Sept. 1984)* ed B Jezowska-Trzebiatowska, J Legendziewicz and W Strek (Singapore: World Scientific)
[41] van Pieterson L, Reid M F, Wegh R T and Meijerink A 2001 *J. Lumin.* **94/95** 79
[42] Dorenbos P 2003 *J. Lumin.* **104** 239
[43] Dorenbos P 2003 *J. Phys.: Condens. Matter* **15** 4797
[44] Nakazawa E and Shiga F 1977 *J. Lumin.* **15** 255
[45] van Pieterson L, Reid M F, Burdick G W and Meijerink A 2002 *Phys. Rev.* B **65** 045114
[46] Kaplyanskii A A and Feofilov P P 1962 *Opt. Spectrosc.* **13** 129
[47] Dorenbos P 2003 *J. Phys.: Condens. Matter* **15** 6249
[48] van Pieterson L, Reid M F, Wegh R T, Soverna S and Meijerink A 2002 *Phys. Rev.* B **65** 045113
[49] Keller S P and Pettit G D 1958 *Phys. Rev.* **111** 1533
[50] Blasse G 1983 *Phys. Status Solidi* a **75** K41
[51] Pei Z and Blasse G 1994 *J. Solid State Chem.* **110** 399
[52] Nakazawa E 1978 *Chem. Phys. Lett.* **56** 161
[53] Nakazawa E 2002 *J. Lumin.* **100** 89
[54] Dujardin C, Kamenskikh I, Ledoux G, Mercier B, Pedrini C and Petrosyan A 2003 *Annual Report* 2002 Deutsches EleKtronen Synchrotron DESY, Hamburg, Germany
[55] Guerassimova N, Garnier N, Dujardin C, Petrosyan A G and Pedrini C 2001 *Chem. Phys. Lett.* **339** 197
[56] Yoshikawa A, Ogino H, Lee J H, Nikl M, Solovieva N, Garnier N, Dujardin C, Lebbou K, Pedrini C and Fukuda T 2003 *Opt. Mater.* **24** 275
[57] Yoshikawa A, Akagi T, Nikl M, Solovieva N, Lebbou K, Dujardin C, Pedrini C and Fukuda T 2002 *Nucl. Instrum. Methods* A **486** 79
[58] Nakazawa E 1979 *J. Lumin.* **18/19** 272
[59] Blasse G 1989 *J. Phys. Chem. Solids* **50** 99
[60] Ryan J L and Jörgensen C K 1966 *J. Phys. Chem.* **70** 2845
[61] Liu X, Zhang Y, Wang Z and Lu S 1988 *J. Lumin.* **40/41** 885
[62] Li Y, Guillen F, Fouassier C and Hagenmuller P 1985 *J. Electrochem. Soc.: Solid State. Techn.* **132** 717
[63] Li Y, Lu H, Li J and Miao X 1986 *J. Lumin.* **35** 107
[64] Gong X, Liu l, Chan W K and Chen W J 2000 *Opt. Mater.* **15** 143
[65] Liang H, Tao Y, Su Q and Wang S 2002 *J. Solid State Chem.* **167** 435
[66] Ropp R C and Carroll B 1977 *J. Phys. Chem.* **81** 746
[67] Liang H, Zeng Q, Tao Y, Wang S and Su Q 2003 *Mater. Sci. Eng.* B **98** 213
[68] Kamenskikh I A, Guerassimova N, Dujardin C, Garnier N, Ledoux G, Pedrini C, Kirm M, Petrosyan A and Spassky D 2003 *Opt. Mater.* **24** 267
[69] Kirm M 2003 private communications
[70] Blasse G and Dirksen G J 1989 *J. Electrochem. Soc.* **136** 1550
[71] Yamashita N and Asano S 1987 *J. Phys. Soc. Japan* **56** 352
[72] Kuzakov S M, Martynovich E F and Parfianovich I A 1977 *Izv. Akad. Nauk SSSR, Ser. Fiz.* **41** 1380
[73] Krämer K W, Güdel H U and Schwartz R N 1997 *Phys. Rev.* B **56** 13830
[74] Ionova G, Krupa J C, Gerard I and Guillaumont R 1995 *New J. Chem.* **19** 677
[75] Krupa J C and Queffelec M 1997 *J. Alloys Compounds* **250** 287
[76] Mazurak Z, Garcia A and Fouassier C 1994 *J. Phys.: Condens. Matter* **6** 2031
[77] Fouassier C, Garcia A and Qing L J 1985 New frontiers in rare earth science and applications *Proc. Int. Conf. on Rare Earth Development and Applications (Beijing, Sept. 1985)* ed G Xu and J Xiao (New York: Academic)
[78] Garcia A, Guillen F and Fouassier C 1985 *J. Lumin.* **33** 15